PRAMANA
— journal of
physics

Vol. 66, No. 4
April 2006
pp. 797–807

Collective flows in high-energy heavy-ion collisions at AGS and SPS energies*

A OHNISHI[1], M ISSE[1], N OTUKA[2], P K SAHU[3] and Y NARA[4]
[1]Division of Physics, Graduate School of Science, Hokkaido University, Sapporo, Hokkaido 060-0810, Japan
[2]Nuclear Data Center, Department of Nuclear Energy System, Japan Atomic Energy Research Institute, Tokai, Ibaraki 319-1195, Japan
[3]Institute of Physics, Sachivalaya Marg, Bhubaneswar 751 005, India
[4]Institut für Theoretische Physik, Johann Wolfgang Goethe-Universität, Robert-Mayer-Str. 10, 60325 Frankfurt am Main, Germany
E-mail: ohnishi@nucl.sci.hokudai.ac.jp

Abstract. Proton collective flows in heavy-ion collisions from AGS ((2–11) A GeV) to SPS ((40, 158) A GeV) energies are investigated in a nonequilibrium transport model with nuclear mean-field (MF). Sideward $\langle p_x \rangle$, directed v_1, and elliptic v_2 flows are systematically studied with different assumptions on the nuclear equation of state (EoS). We find that momentum dependence in the nuclear MF is important for understanding the proton collective flows at AGS and SPS energies. Calculated results with momentum-dependent MF qualitatively reproduce the experimental data of proton sideward, directed, and elliptic flows in an incident energy range of (2–158) A GeV.

Keywords. Collective flow; heavy-ion collision; equation of state.

PACS Nos 25.75.Ld; 24.10.-i; 25.75.-q

1. Introduction

Nuclear equation of state (EoS) is important not only in nuclear physics but also in astrophysics and particle physics. At around the saturation density, EoS gives the bulk properties of nuclei such as the binding energy and the radius. While first principle lattice QCD simulations are possible for hot baryon-free nuclear matter, phenomenological studies are necessary to connect the experimental heavy-ion collision data with the EoS especially for nuclear matter at finite baryon densities. As a result, determining EoS has been one of the largest motivations of heavy-ion physics in these decades [2–21]. In high-energy heavy-ion collisions, where nuclear

*This talk is based on ref. [1]

matter in a wide range of temperatures and densities are probed, many ideas on the EoS and phases have been examined. For example, very dense matter is created in recent RHIC experiments [22] suggesting the creation of the gas of deconfined quarks and gluons (QGP).

Since the first prediction [2] and experimental observation [3] of collective flows, their relation to EoS has been extensively discussed. Strong collective flows were first considered to be the evidence of hard EoS [4], but later on, the effects of momentum-dependent mean-field was found to be important [4,5]. In order to distinguish the momentum and density dependence, we need to invoke heavy-ion collision data in a wide incident energy range, and now we have systematic collective flow data at various incident energies; LBNL-Bevalac [6], GSI-SIS [7], BNL-AGS [8–11], CERN-SPS [12], and BNL-RHIC [23].

Collective flow data obtained at AGS energies ((2–11) A GeV) show a good landmark to determine EoS. It was demonstrated in RBUU that we can explain all the radial, sideward, and elliptic flows at AGS energies with EoS with $K \sim 300$ MeV if we take into account the saturating momentum dependence of the mean-field (MF), a large number of hadronic resonances, and string degrees of freedom [13]. Recently, Danielewicz *et al* have also discussed the EoS with these data within Boltzmann equation simulation [11,14,15], showing that reliable stiffness value ($K =$ 167–380 MeV) cannot be uniquely determined from currently available collective flow data (F or v_2) up to AGS energies. These two works do not necessarily provide the same conclusion for the stiffness. In order to reduce these ambiguities and to pin down the EoS more precisely, recently measured flow data at lower SPS energies ((20–80) A GeV) may be helpful, because higher baryon density would be reached at these incident energies.

We have recently investigated collective flows from 2 A GeV to 158 A GeV [1] by using a hadronic cascade model (JAM) [24] combined with a covariant prescription of MF (RQMD/S) [25]. In this proceedings, we show the results of proton flows based on ref. [1].

2. Nonequilibrium transport model and the equations of state

Heavy-ion collision is a dynamical process of a system in which the temperature and density are not uniform and the equilibrium is not necessarily reached. While hydrodynamical description is the most direct way to connect the EoS and dynamics and its successes at RHIC, nonequilibrium effects are more important at SPS energies and nonequilibrium dynamics is required to study the EoS of dense nuclear matter through heavy-ion collisions.

Hadron-string cascade processes are the main source of thermalization and particle production up to SPS energies. By increasing incident energy from AGS ((2–11)A GeV) to SPS ((20–158)A GeV), the main particle production mechanism in hadron–hadron collisions evolves from resonance productions to string formations. At higher energies, hard partonic interaction (jet production) becomes more important, and the jet production cross-section reaches around 20% of the total cross-section of pp at RHIC [26]. JAM includes all these particle production mechanisms, and the applicable incident energy range is expected to be enough. Readers can find detailed explanation of JAM in ref. [24].

Table 1. Mean field parameter set.

Type	α (MeV)	β (MeV)	γ	$C_{\rm ex}^{(1)}$ (MeV)	$C_{\rm ex}^{(2)}$ (MeV)	μ_1 (fm^{-1})	μ_2 (fm^{-1})	K (MeV)
MH	−33	110	5/3	−277	663	2.35	0.4	448
MS	−268	345	7/6	−277	663	2.35	0.4	314
H	−124	70.5	2	–	–	–	–	380
S	−356	303	7/6	–	–	–	–	200

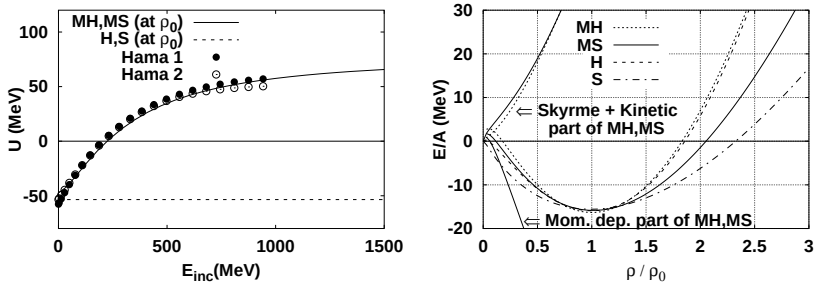

Figure 1. Left: Momentum dependence of the single particle potentials for momentum-dependent hard (MH), soft (MS) as well as momentum-independent hard (H) and soft (S) are compared with the real part of the global Dirac optical potential by Hama *et al.* Right: Density dependence of total energy per nucleon for momentum-dependent (MH, MS) and independent (H, S) potentials.

It is necessary to include MF effects to explain collective flow data, and the MF should depend on momentum as well as density in order to describe flows in a wide incident energy range. We adopt here a simple Skyrme-type density-dependent MF in the zero-range approximation, and a Lorentzian-type momentum-dependent MF [5] which simulates the exchange term (Fock term) of the Yukawa potential. Single particle potential U then has the form

$$U(\mathbf{r},\mathbf{p}) = \frac{\alpha\rho(\mathbf{r})}{\rho_0} + \frac{\beta\rho(\mathbf{r})^\gamma}{\rho_0^\gamma} + \sum_{k=1,2} \frac{C_{\rm ex}^{(k)}}{\rho_0} \int \mathrm{d}\mathbf{p}' \frac{f(\mathbf{r},\mathbf{p}')}{1+[(\mathbf{p}-\mathbf{p}')/\mu_k]^2}. \qquad (1)$$

This MF potential is derived from the total potential energy, through a relation $U = \delta V/\delta f$. Parameters α, β and γ in eq. (1) are determined to reproduce the saturation of the total energy per nucleon at the normal nuclear density, i.e. $E/A|_{\rho=\rho_0} = -16$ MeV, and $P = \rho^2\partial(E/A)/\partial\rho|_{\rho=\rho_0} = 0$ MeV/fm^3 [27]. The incompressibility K is obtained from $K = 9\rho^2\partial^2(E/A)/\partial\rho^2|_{\rho=\rho_0}$. Parameters for hard (H) and soft (S) EoS are listed in table 1 and the density dependences of the total energy per nucleon are shown in the right panel of figure 1.

Parameters $C_{\rm ex}^{(k)}$ and μ_k are taken to reproduce the real part of the global Dirac optical potential (Schrödinger equivalent potential) of Hama *et al* [28], in which angular distribution and polarization quantities in proton–nucleus elastic scatterings are analyzed in the range of 10 MeV–1 GeV in Dirac phenomenology. Single

particle potential at $\rho = \rho_0$ is compared to the Schrödinger equivalent potential in ref. [28] in the left panel of figure 1. Parameters for the momentum-dependent potentials are shown as MH and MS in table 1. These parameter sets are based on ref. [29] with some simplifications. We have fixed the high energy limit of the optical potential, $U \to 77$ MeV at $E_{\rm inc} \to \infty$, leading to a constraint $\alpha + \beta = 77$ MeV. This constraint generally makes EoS stiffer compared to those in ref. [16].

We include the above MF effects into JAM [24] by means of simplified RQMD (RQMD/S) [25] framework. The relativistic quantum molecular dynamics (RQMD) [30,31] is a constraint Hamiltonian dynamics, in which potentials are treated in a covariant way. RQMD/S [25] uses much simpler and more practical time fixation constraints compared to the original one [30,31].

In this work, we take into account potential interactions only between nucleons (protons and neutrons). MF for other hadrons (baryon resonances, anti-baryons, mesons, resonances, etc.) are ignored. Simulation time step size is taken to be $\mathrm{d}t = 0.1$ fm/c at all incident energies.

3. Collective flows from AGS to SPS energies

When two heavy nuclei collide at high energies at finite impact parameters, pressure gradient is anisotropic in the initial stages of a collision. As a result, it generates anisotropic collective flows. Up to now, several kinds of collective flows are proposed to probe high dense matter. The first one is the sideward flow (also called directed flow) $\langle p_x \rangle$, which is defined as the mean value of p_x, where x is defined as the impact parameter direction on the reaction plane. Sideward flow is mainly generated by the participant–spectator interactions. Nucleons in the projectile feel repulsive interaction from the target nucleus during the contact time of the projectile and the target. This repulsion pushes projectile nucleons out in the positive sideward direction if the contact time is long enough. When the incident energy is very high, contact time in collisions becomes shorter due to the Lorentz contraction. Therefore sideward flow decreases. At SPS energies, other types of collective flows, called directed (v_1) and elliptic (v_2) flows, are mainly measured. These are defined as the nth Fourier coefficient,

$$\frac{\mathrm{d}^3N}{p_{\rm T}\mathrm{d}p_{\rm T}\mathrm{d}y\mathrm{d}\phi} = \frac{\mathrm{d}^2N}{2\pi p_{\rm T}\mathrm{d}p_{\rm T}\mathrm{d}y}\left(1 + \sum_n 2v_n(p_{\rm T}, y)\cos n\phi\right), \tag{2}$$

where the azimuthal angle ϕ is measured from the reaction plane. The directed flow v_1 and the elliptic flow v_2 are the first and second Fourier coefficients of the azimuthal distribution, respectively,

$$v_1 = \langle \cos\phi \rangle = \langle p_x/p_{\rm T} \rangle, \quad v_2 = \langle \cos 2\phi \rangle = \langle (p_x^2 - p_y^2)/p_{\rm T}^2 \rangle. \tag{3}$$

These collective flows are reviewed in ref. [32].

The effects of MF in high-energy heavy-ion collisions are visible but not very large in single-particle spectra, such as rapidity distribution $\mathrm{d}N/\mathrm{d}y$ or transverse mass distribution $\mathrm{d}^2N/m_{\rm T}\mathrm{d}m_{\rm T}\mathrm{d}y$. In this section, we demonstrate that MF effects are essential to study anisotropic collective flows in the hadron-string transport model JAM with MF potentials.

3.1 *Collective flows at AGS energies*

We show proton sideward flow $\langle p_x \rangle$ in mid-central Au+Au collisions at AGS energies ($E_{\rm inc}$ =(2–11) A GeV) together with AGS-E895 [10] and AGS-E877 [8] data in figure 2. We choose the impact parameter range $4 < b < 8$ fm in the calculations which roughly corresponds to mid-central collisions in experimental data. It is seen that both cascade and momentum-independent MF results are inconsistent with the data at $E_{\rm inc} \leq 4$ A GeV. The magnitude of $\langle p_x \rangle$ in forward rapidity region ($y/y_{\rm proj} \simeq \pm 1$) is small compared to the data, and the slope parameters at mid-rapidity are also smaller than that of the data. The momentum-independent MF reduces $\langle p_x \rangle$ in forward rapidity region, and enhances the slope parameters at mid-rapidity. The former is an unfavorable effect in explaining the data, and the latter is not enough.

Proton sideward flow data are well-reproduced with the momentum-dependent MF. The momentum-dependent MF pushes up the flow linearly as a function of rapidity, and it becomes consistent with the data. As the incident energy increases, MF effects on the slope parameter at mid-rapidity become small, but we can still see clear differences at forward rapidities between the results with and without momentum dependence.

Our results suggest the necessity of the momentum dependence in the MF to give large magnitude emission to x direction at forward rapidity and also the slope at mid-rapidity. We note that our results with momentum-dependent MF are consistent with the previous calculations with MF on the collective flow data at AGS [13,15,18] as well as SIS energies [7,20].

The importance of the momentum dependence in the MF is more clearly seen in the transverse momentum dependence of the proton elliptic flow v_2 as shown in figure 3. Only if momentum dependence is included, we reproduce the consistent behavior of the $p_{\rm T}$ dependence as well as the energy dependence.

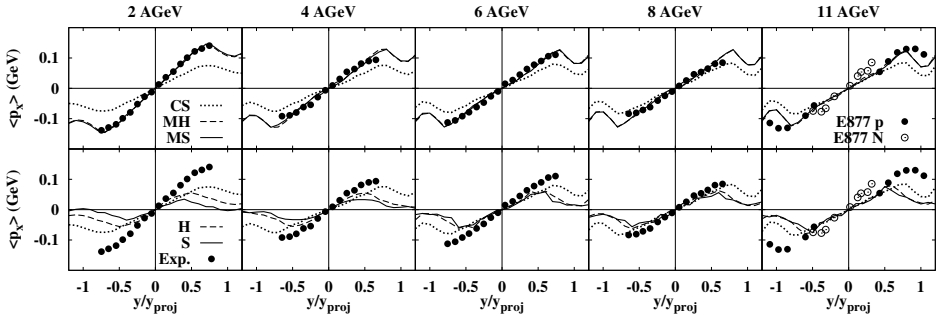

Figure 2. Sideward flows $\langle p_x \rangle$ of protons in mid-central Au+Au collisions at (2–11) A GeV are compared to the AGS-E895 and AGS-E877 data. Lines show the calculated results of cascade with momentum-dependent hard/soft mean-field (MH/MS), cascade with momentum-independent mean-field (H/S) and cascade without mean-field (CS).

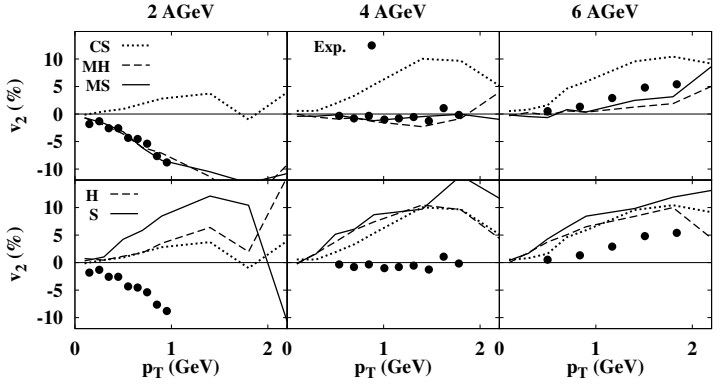

Figure 3. Transverse momentum dependence of the elliptic flow v_2 for protons in Au+Au mid-central collisions at (2,4,6) A GeV are compared to AGS-E895 data.

3.2 *Collective flows at SPS energies*

In figure 4, we show the collective flows v_1 and v_2 as a function of rapidity and transverse momentum in comparison with the data in mid-central Pb+Pb collisions at $E_{\rm inc} = 40$ A GeV and 158 A GeV by CERN-NA49 Collaboration [12]. Generally it is found that momentum-dependent MF generally improves the description of v_1 and v_2.

In the rapidity dependence of v_1 (upper left panel of figure 4), it is interesting to note that the cascade model overestimates v_1 for protons contrary to the underestimate of $\langle p_x \rangle$ at AGS energies. We also see that v_1 is reduced at SPS energies with momentum-dependent MF, while $\langle p_x \rangle$ is enhanced at AGS energies. This is a reverse behavior compared to that at lower incident energies. Note also that the results with momentum-independent MF predict larger v_1 than that of the cascade results. Large v_1 values at large rapidities ($y \sim 2.0$) in the calculated results come from nucleons in the spectator fragments. Another interesting point is the 'wiggle' (a negative slope of the proton v_1 near mid-rapidity) [12,19] at 158 A GeV, which we do not see at lower incident energies. This wiggle cannot be explained with either cascade or with momentum-independent MF. The wiggle behavior appears only in the calculated results with momentum-dependent MF.

Transverse momentum dependence of v_1 for protons (upper right panel of figure 4) at 158 A GeV is very different from that at 40 A GeV. Dense baryonic matter is tentatively formed in the calculations up to around 40 A GeV, while many strings are formed and hadrons are formed later at 158 A GeV at mid-rapidity. As a result, v_1 does not necessarily grow as a function of $p_{\rm T}$ at 158 A GeV, because strings do not feel MF in our model, and hadrons with large $p_{\rm T}$ from string decay have long formation time in the total CM system, and they would have smaller chances to interact with other hadrons before strings decay. It is important to notice that the difference of the stiffness in EoS leads to 10–30% difference on the prediction of $v_1(p_{\rm T})$. This suggests a possibility to determine the stiffness of the EoS using transverse momentum dependence of the proton directed v_1 flows.

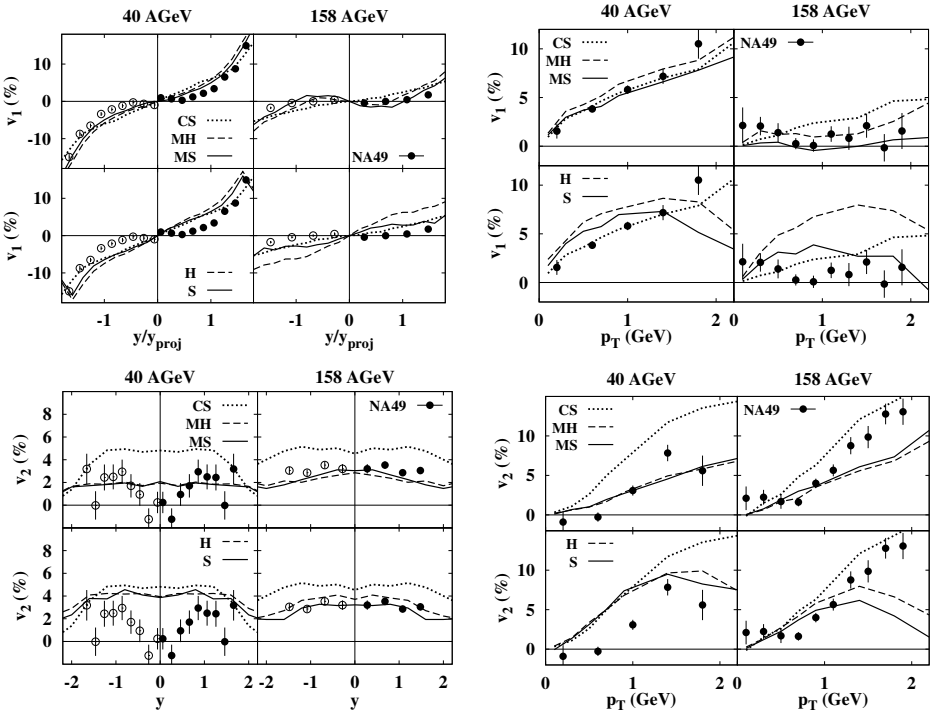

Figure 4. Proton directed v_1 (upper) and elliptic v_2 (lower) flows as a function of rapidity (left) and transverse momentum (right) in mid-central Pb+Pb collisions at $E_{\rm inc} = 40$ A GeV and 158 A GeV in comparison with SPS-NA49 data. Lines show the calculated results of cascade with momentum-dependent hard/soft mean-field (MH/MS), cascade with momentum-independent mean-field (H/S) and cascade without mean-field (CS).

The rapidity dependence of v_2 for protons (lower left panel of figure 4) shows that all types of MF suppress the v_2 in almost all the rapidity region. Especially, in the case of momentum-dependent MF, proton elliptic flows are suppressed by more than a factor of two compared to the cascade results.

Our result on $v_2(y)$ does not have the collapse at mid-rapidity that is seen in the NA49 data. This may be a strong indication of a first-order phase transition at high baryon densities achieved in the Pb+Pb collisions at 40 A GeV [21]. However, since the experimental results strongly depend on the analysis method (reaction plane, two- and four-particle correlation) [12], at present we do not think that the dip is an evidence of the first-order phase transition.

In the transverse momentum dependence of v_2 for protons (right bottom panel of figure 4), all the models show approximate linear $p_{\rm T}$ dependence of $v_2(p_{\rm T})$, and the slope of the proton $v_2(p_{\rm T})$ is well-explained at low $p_{\rm T}$ with the momentum-dependent MF. On the other hand, it is seen that v_2 is insensitive to the stiffness of the EoS. Without momentum dependence, MF effects are not strong enough to

suppress v_2, and strong repulsion effect from momentum dependence is needed to get larger suppression in order to explain the data. This suggests that momentum dependence in the baryon MF is crucial for understanding the proton collective flow v_2 at SPS energies.

We now turn to the discussion of the difference between v_1 and v_2. We have shown that MF effects on v_2 is strong, but it is insensitive to the incompressibility of the EoS at SPS energies within our approach. On the other hand, rather visible effect on the incompressibility has been seen in v_1. This may come from the difference of developing time between v_1 and v_2, i.e. v_2 is formed until the time reaches the order of nuclear radius, while v_1 may be determined in the earliest stage of the collision, where baryon density is the highest in the collision. The directed flow v_1 is mainly generated by the interaction between participants and spectators, and spectators go away very fast at high energies. On the other hand v_2 is not formed in the earliest stage of the collision in our model. This is because our current hadronic transport approach does not have large participant pressure in the early stages of the collisions, as we do not explicitly include MF for strings and partonic interactions. In a hydrodynamic picture, v_2 develops from very early times due to thermal pressure. This is a striking difference between our approach and hydrodynamics as previously studied in ref. [30].

3.3 *Elliptic flow excitation functions from AGS to SPS energies*

When the incident energy is not high enough, spectators squeeze participants out of the reaction plane due to the repulsive nuclear interactions at $0.2 \lesssim E_{\rm inc} \lesssim 4$ A GeV. This squeezing leads to a negative value of the elliptic flow of nucleons ($v_2 < 0$). The elliptic flow, therefore, shows the strength of the repulsive interaction at lower energies. On the other hand, elliptic flow becomes positive at higher energies, because there is no such squeezing effect due to the Lorentz contraction. Elliptic flow gives information about how much pressure is generated at higher energies.

In figure 5, we show the incident energy dependence of the proton elliptic flow v_2 in mid-central collisions with measured data ($-0.1 < y < 0.1$ for AGS, $0 < y < 2.1$ ($0 < y < 1.8$) for SPS 158 A (40 A) GeV) [9,12]. Rapidity cut $|y| < 0.2y_{\rm proj}$ has been used in calculations. Experimental data clearly show the evolution from squeezing to almond-shaped participant dynamics. With both cascade and momentum independent MF (H, S), we cannot explain strong squeezing effects at lower energies, and the calculated v_2 values are generally larger than the data at all incident energies. Momentum-dependent MF (MH, MS), which is repulsive in the incident energy range under consideration, pushes down the elliptic flow significantly. We qualitatively reproduce the incident energy dependence from AGS [9] to SPS [12] energies.

Calculated results with both MH and MS are smooth as a function of beam energy, while the data at $E_{\rm inc} = 40$ A GeV has a dip [12]. Confirmation of data is necessary to examine the incident energy dependence of v_2, whether it is a monotonic function or has a dip at around $E_{\rm inc} \sim 40$ A GeV by looking at the missing data points.

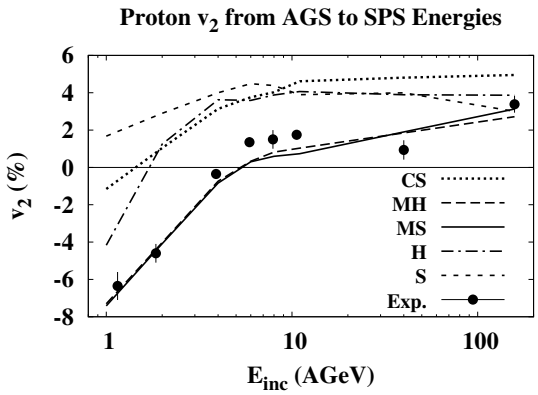

Figure 5. Incident energy dependence of proton elliptic flow at mid-rapidities in mid-central heavy-ion collisions from 1 A GeV to 158 A GeV. Lines show the results of model calculations. The experimental data are taken from LBL-EOS, AGS-E895, E877, and SPS-NA49.

4. Summary

We have investigated collective flows in heavy-ion collisions from AGS ((2–11) A GeV) to SPS ((40, 158) A GeV) energies by using a combined framework of hadron-string cascade (JAM) [24] and covariant constraint Hamiltonian dynamics (RQMD/S) [25]. In JAM, various particle production mechanisms are taken into account, and momentum dependence of the MF is fitted [29] to the data [28]. Calculated results are compared with the data of sideward $\langle p_x \rangle$, directed v_1, and elliptic v_2 flows as a function of rapidity, transverse momentum and beam energy from AGS to SPS. Generally, results with momentum-dependent MF reasonably explain the trend of the data for proton flows. We note that it is for the first time to explain anisotropic proton collective flow data of heavy-ion collisions from AGS to SPS in one framework consistently. Momentum dependence of MF is found to be very important to explain several important features of collective flow data at AGS and SPS energies.

It would be still premature to determine the nuclear EoS. In ref. [1], we have discussed the model uncertainties in detail. Especially, we have discussed the reason why the EoS dependence of collective flows is small in the present model. Our conclusion is that the present model is essentially a Lorentz scalar potential model, in which potential effects are largely suppressed at high energies. Clarification of the model dependence of the MF treatment is an imporant task to be done.

Acknowledgements

We are grateful to Profs Tomoyuki Maruyama and Pawel Danielewicz for useful discussions and comments. This work is supported in part by the Ministry of Education, Science, Sports and Culture, Grand-in-Aid for Scientific Research (C)(2), No. 15540243, 2003.

References

[1] M Isse, A Ohnishi, N Otuka, P K Sahu and Y Nara, *Phys. Rev.* **C72**, 064908 (2005), arXiv:nucl-th/0502058
[2] J Kapusta and D Strottman, *Phys. Lett.* **B106**, 33 (1981)
H Stöcker *et al*, *Phys. Rev.* **C25**, 1873 (1982)
[3] H A Gustafsson *et al*, *Phys. Rev. Lett.* **52**, 1590 (1984)
[4] G F Bertsch and S Das Gupta, *Phys. Rep.* **160**, 189 (1988)
[5] C Gale, G F Bertsch and S Das Gupta, *Phys. Rev.* **C35**, 1666 (1987)
G M Welke *et al*, *Phys. Rev.* **C38**, 2101 (1988)
L P Csernai, G Fai, C Gale and E Osnes, *Phys. Rev.* **C46**, 736 (1992)
[6] EOS Collaboration: J Chance *et al*, *Phys. Rev. Lett.* **78**, 2535 (1997)
J C Kintner *et al*, *Phys. Rev. Lett.* **78**, 4165 (1997)
K G R Doss *et al*, *Phys. Rev. Lett.* **57**, 302 (1986)
[7] FOPI Collaboration: N Bastid *et al*, *Nucl. Phys.* **A622**, 573 (1997)
FOPI Collaboration: A Andronic *et al*, *Phys. Rev.* **C67**, 034907 (2003)
FOPI Collaboration (G Stoicea *et al*) and P Danielewicz, *Phys. Rev. Lett.* **92**, 072303 (2004)
[8] E877 Collaboration: J Barrette *et al*, *Phys. Rev.* **C55**, 1420 (1997); **56**, 3254 (1997)
[9] E895 Collaboration: C Pinkenburg *et al*, *Phys. Rev. Lett.* **83**, 1295 (1999)
[10] E895 Collaboration: H Liu *et al*, *Phys. Rev. Lett.* **84**, 5488 (2000)
[11] E895 Collaboration (P Chung *et al*) and P Danielewicz, *Phys. Rev.* **C66**, 021901(R) (2002)
E895 Collaboration: J L Klay *et al*, *Phys. Rev. Lett.* **88**, 102301 (2002)
[12] NA49 Collaboration: C Alt *et al*, *Phys. Rev.* **C68**, 034903 (2003)
[13] P K Sahu, W Cassing, U Mosel and A Ohnishi, *Nucl. Phys.* **A672**, 376 (2000)
[14] P Danielewicz *et al*, *Phys. Rev. Lett.* **81**, 2438 (1998)
[15] P Danielewicz, *Nucl. Phys.* **A673**, 375 (2000)
P Danielewicz, R Lacey and W G Lynch, *Science* **298**, 1592 (2002)
[16] A B Larionov, W Cassing, C Greiner and U Mosel, *Phys. Rev.* **C62**, 064611 (2000)
[17] T Maruyama, W Cassing, U Mosel, S Teis and K Weber, *Nucl. Phys.* **A573**, 653 (1994)
[18] P K Sahu and W Cassing, *Nucl. Phys.* **A712**, 357 (2002)
[19] R J M Snellings *et al*, *Phys. Rev. Lett.* **84**, 2803 (2000)
[20] D Persram and C Gale, *Phys. Rev.* **C65**, 064611 (2002)
[21] H Stöcker, E L Bratkovskaya, M Bleicher, S Soff and X Zhu, arXiv:nucl-th/0412022
[22] See, for example, *Nucl. Phys.* **A698** (2002) and references therein
[23] STAR Collaboration: C Adler *et al*, *Phys. Rev.* **C66**, 034904 (2002)
PHOBOS Collaboration: B B Back *et al*, *Phys. Rev. Lett.* **89**, 222301 (2002)
PHENIX Collaboration: S S Adler *et al*, *Phys. Rev. Lett.* **91**, 182301 (2003)
STAR Collaboration: J Adams *et al*, *Phys. Rev. Lett.* **92**, 062301 (2004)
[24] Y Nara, N Otuka, A Ohnishi, K Niita and S Chiba, *Phys. Rev.* **C61**, 024901 (2000)
[25] T Maruyama *et al*, *Prog. Theor. Phys.* **96**, 263 (1996)
[26] X-N Wang and M Gyulassy, *Phys. Rev.* **D44**, 3501 (1991)
[27] J Aichelin *et al*, *Phys. Rev. Lett.* **58**, 1926 (1987)
[28] S Hama *et al*, *Phys. Rev.* **C41**, 2737 (1990)
[29] T Maruyama *et al*, *Phys. Rev.* **C57**, 655 (1998)
[30] H Sorge, H Stöcker and W Greiner, *Ann. Phys.* **192**, 266 (1989)
H Sorge, *Phys. Rev.* **C52**, 3291 (1995)
H Sorge, *Phys. Lett.* **B402**, 251 (1997); *Phys. Rev. Lett.* **82**, 2048 (1999)

[31] T Maruyama *et al*, *Nucl. Phys.* **A534**, 720 (1991)
[32] J-Y Ollitrault, *Nucl. Phys.* **A638**, 195c (1998)

Note added in proof

After submitting this proceedings paper, we found a numerical problem in the program and changed several model parameters and assumptions in the results shown in ref. [1], where MF for all baryons are included after their formation time. While the conclusion is the same as that in this proceedings paper, MF effects to the elliptic flow at SPS energies are found to be smaller since we switched off the MF during the formation time.